

# ELASTIC $pp$ SCATTERING AT LHC ENERGIES

C. Merino\* and Yu.M. Shabelski\*\*

\* Departamento de Física de Partículas, Facultade de Física  
and Instituto Galego de Física de Altas Enerxías  
Universidade de Santiago de Compostela  
Santiago de Compostela 15782  
Galiza, Spain  
E-mail: merino@fpaxp1.usc.es

\*\* Petersburg Nuclear Physics Institute  
Gatchina, St.Petersburg 188350, Russia  
E-mail: shabelsk@thd.pnpi.spb.ru

We consider the first LHC data for elastic  $pp$  scattering in the framework of Regge theory with multiple Pomeron exchanges. The simplest eikonal approach allows one to describe differential elastic cross sections at LHC, as well as  $pp$  and  $\bar{p}p$  scattering at lower collider energies, on a reasonable level.

PACS. 25.75.Dw Particle and resonance production

# 1 Introduction

In Regge theory the Pomeron exchange dominates the high energy soft hadron interaction. The Pomeron has vacuum quantum numbers, so the difference in  $pp$  and  $\bar{p}p$  should disappear. At LHC energies the contributions of all other exchanges to the elastic scattering amplitude becomes negligible, and then one can directly extract the Pomeron parameters from the experimental data.

In the present paper we consider the first LHC data (TOTEM Collaboration [1]) for  $pp$  small angle elastic scattering and we compare them with the simplest approaches of Regge theory and with the results obtained for other lower collider energies.

The experimental elastic cross section is well described by a pure exponential form in the interval of momentum transfer  $|t| = 0 - 0.3 \text{ GeV}^2$ . In this interval the cross section falls down more than 400 times. The experimental ratio of  $\sigma_{el}/\sigma_{tot}$  is equal to  $\sim 0.25$  and an interesting point to be analysed is whether in the framework of a conventional Regge theory we have a chance to describe such a large elastic cross section without introducing, either a second Pomeron pole with a large intercept  $\alpha_P(0) = 1.362$ , as in [2], a rather non-trivial spatial  $b_t$ -distribution of the matter in the proton with a deep minimum at  $b_t = 0$ , like it was done in [3] (see the form of  $\gamma(b)$  in Eq. (9) of [3])<sup>1</sup>, or more complicated approaches, such as the three-channel eikonal model [4] or the model [5] in which uses the general parton distributions.

## 2 Elastic Scattering Amplitude at LHC energies

Let us consider elastic  $pp$  ( $\bar{p}p$ ) scattering at very high energies in the framework of Regge-Gribov theory [6], where only Pomeron exchanges should be accounted for. It is suitable to use the following normalization of the elastic scattering amplitude  $A(s, t)$ :

$$\sigma^{tot} = 8\pi \cdot \text{Im}A(s, t = 0) , \quad \frac{d\sigma}{dt} = 4\pi \cdot |A(s, t)|^2 . \quad (1)$$

The simplest contribution to the elastic scattering amplitude is the one-Pomeron,  $P$ , exchange, that can be written as:

$$A^{(1)}(s, t) = \gamma(t) \cdot \left( \frac{s}{s_0} \right)^{\alpha_P(t)-1} \cdot \eta(\Theta) , \quad (2)$$

---

<sup>1</sup>Note that the total cross section obtained in [3] for  $\sqrt{s} = 7 \text{ TeV}$  is  $\sigma_{tot} = 90.9 \text{ mb}$ , much smaller than that measured by TOTEM.

where  $\gamma(t) = g_1(t) \cdot g_2(t)$ ,  $g_1(t)$  and  $g_2(t)$  are the couplings of a Pomeron to the beam and target hadrons,  $\alpha_P(t) = \alpha_P(0) + \alpha'_P \cdot t$  is the Pomeron trajectory,  $\alpha_P(0)$  (intercept) and  $\alpha'_P$  (slope) are some numbers, and  $\eta(\Theta)$  is the signature factor which determines the complex structure of the scattering amplitude ( $\Theta$  equal to  $+1$  and to  $-1$  for Reggeon with positive and negative signature, respectively). Specifically for Pomeron exchange ( $\Theta = +1$ ):

$$\eta(\Theta) = \frac{1 + \Theta \cdot \exp[-i\pi\alpha_P(t)]}{\sin[\pi\alpha_P(t)]} = i - \tan^{-1} \left( \frac{\pi\alpha_P(t)}{2} \right). \quad (3)$$

In the case of a Pomeron trajectory with  $\alpha_P(0) > 1$ , the correct asymptotic behavior  $\sigma_{tot} \sim \ln^2 s$  [7, 8] compatible with the Froissart bound [9], can only be obtained by taking into account the multipomeron cuts.

Indeed, for the Pomeron trajectory

$$\alpha_P(t) = 1 + \Delta + \alpha'_P \cdot t, \quad \Delta > 0, \quad (4)$$

the one-Pomeron contribution to  $\sigma_{hN}^{tot}$  rises with energy as  $s^\Delta$ . To comply with the  $s$ -channel unitarity and, in particular, with the Froissart bound, this contribution should be screened by the multipomeron discontinuities shown in Fig. 1.

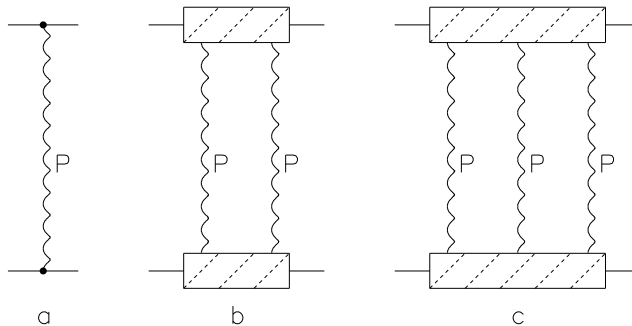


Figure 1: Regge-pole theory diagrams: (a) single, (b) double, and (c) triple Pomeron exchange in elastic  $pp$  scattering.

A simple quasi-eikonal treatment [10] allows one to present the total elastic scattering amplitude  $A(s, t)$  as a series

$$A(s, t) = A^{(1)}(s, t) + A^{(2)}(s, t) + A^{(3)}(s, t) + \dots, \quad (5)$$

where each  $A^{(n)}(s, t)$  contribution corresponds to the exchange of  $n$  Pomerons. The value of  $A^{(1)}(s, t)$  is given by Eq. (2), and

$$A^{(2)}(s, t) = \frac{1}{2!} \int \frac{d^2\vec{q}_1}{\pi} \cdot A^{(1)}(s, \vec{q}_1) \cdot i \cdot A^{(1)}(s, \vec{q} - \vec{q}_1) \quad (6)$$

$$A^{(3)}(s, t) = \frac{1}{3!} \int \frac{d^2 \vec{q}_1}{\pi} \cdot \frac{d^2 \vec{q}_2}{\pi} \cdot A^{(1)}(s, \vec{q}_1) \cdot i \cdot A^{(1)}(s, \vec{q}_2) \cdot i \cdot A^{(1)}(s, \vec{q} - \vec{q}_1 - \vec{q}_2), \quad (7)$$

where all  $q_i$  are two-dimensional vectors in the perpendicular plane to the beam axis,  $t = -\vec{q}^2$ .

The results of the integrations in Eqs. (6), (7), etc., depend on the assumption about the form of the function  $\gamma(t)$ , with  $t = -q^2$ . These integrations can be analytically performed in the simplest case of Gaussian functions:

$$\gamma(q^2) = \gamma_0 \cdot e^{-R^2 \cdot q^2}. \quad (8)$$

In this case the total elastic scattering amplitude of Eq. (5) is equal to

$$A(s, t) = \eta_P \cdot \gamma_0 \cdot e^{\Delta \xi} \cdot \sum_{n=1}^{\infty} \frac{1}{n \cdot n!} \left( i \cdot C \cdot \frac{\eta_P \cdot (q^2/n^2) \cdot \gamma_0}{\lambda} \cdot e^{\Delta \cdot \xi} \right)^{n-1} \cdot \exp \left[ -\frac{\lambda}{n} q^2 \right], \quad (9)$$

where  $C$  is the quasi-eikonal enhancement coefficient (see [10]),  $\lambda = R^2 + \alpha'_P \cdot \xi$ ,  $\xi = \ln s/s_0$ ,  $s_0 = 1 \text{ GeV}^2$ .

At asymptotically high energies,  $s \rightarrow \infty$ , the amplitude of Eq. (9) leads to the Froissart behaviour of the total cross section,  $\sigma^{tot}(s) \sim \ln^2 s$ .

On the other hand, it is well-known that the form of the function  $\gamma(q^2)$  in Eq. (8) is in contradiction with the experimental data on the shape of the differential elastic cross section, so we have also used the parametrization of  $\gamma(q^2)$  as a sum of two gaussians:

$$\gamma(q^2) = \gamma_0 \cdot (a \cdot e^{-R_1^2 \cdot q^2} + (1 - a) \cdot e^{-R_2^2 \cdot q^2}), \quad (10)$$

that leads to a better agreement with the data.

### 3 Comparison with the experimental data

The results of the calculation of  $d\sigma/dt$  at  $\sqrt{s} = 7 \text{ TeV}$ , obtained with the one-exponential parametrization of  $\gamma(q^2)$  in Eq. (8), are presented in Fig. 2. The values of  $\gamma_0$  were fixed by the value of  $\sigma^{tot}$  at the same energy measured by TOTEM Collaboration [1]. The two theoretical curves correspond to the values  $C = 1.5$  (quasi-eikonal approach) and  $C = 1$  (eikonal approach), and both are in total disagreement with the experimental data (several experimental points presented in Fig. 2 are taken from [12]).

The main reason of the disagreements of the two theoretical curves in Fig. 2 with the experimental data comes from the rather large rescattering contributions (exchanges

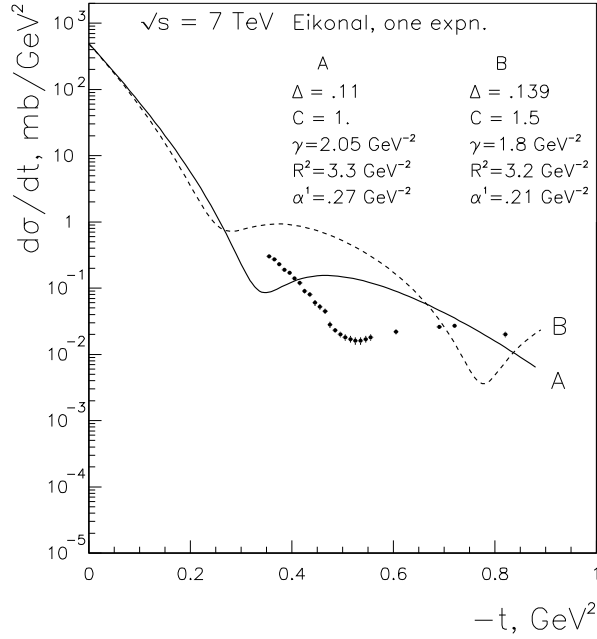


Figure 2: The differential cross section of elastic  $pp$  scattering at  $\sqrt{s} = 7$  TeV calculated in both eikonal (A) and quasi-eikonal (B) approaches, with the one-exponential parametrization of  $\gamma(q^2)$  in Eq. (8). The experimental points are taken from [12].

of several Pomerons) in Eq. (9). These contributions transform the bare Gaussian  $t$ -dependence of  $d\sigma/dt$  given by Eq. (8) into functions faster decreasing with  $q^2$ , whereas the experimental LHC data [1, 12] practically show a Gaussian  $t$ -dependence.

The simplest way to avoid this problem is to use a two-exponential form for the function  $\gamma(q^2)$  as the one given by Eq. (10). All the integrals in Eqs. (6), (7), etc., can be analytically calculated, giving an expression for  $A^{(n)}$ :

$$\begin{aligned}
A^{(n)}(s, q^2) &= \frac{i^{(n-1)}}{n!} \cdot [\eta_P \cdot (q^2/n^2) \cdot \gamma_0 e^{\Delta \cdot \xi}]^n \cdot \left[ \frac{a^n}{n \cdot \lambda_1^{(n-1)}} + \frac{(a-1)^n}{n \cdot \lambda_2^{(n-1)}} + \right. \\
&+ \sum_{k=1}^{n-1} C_n^k \cdot \frac{a^{(n-k)} \cdot (1-a)^k}{\lambda_1^{(n-k-1)} \cdot \lambda_2^{(k-1)} \cdot [k \cdot \lambda_1 + (n-k) \cdot \lambda_2]} \cdot \\
&\cdot \left. \exp\left(-\frac{q^2}{(n-k) \cdot \beta_1 + k \cdot \beta_2}\right) \right], \\
C_n^k &= \frac{n!}{k! \cdot (n-k)!}, \quad \lambda_i = R_i^2 + \alpha'_P \cdot \xi, \quad \beta_i = 1/\lambda_i.
\end{aligned} \tag{11}$$

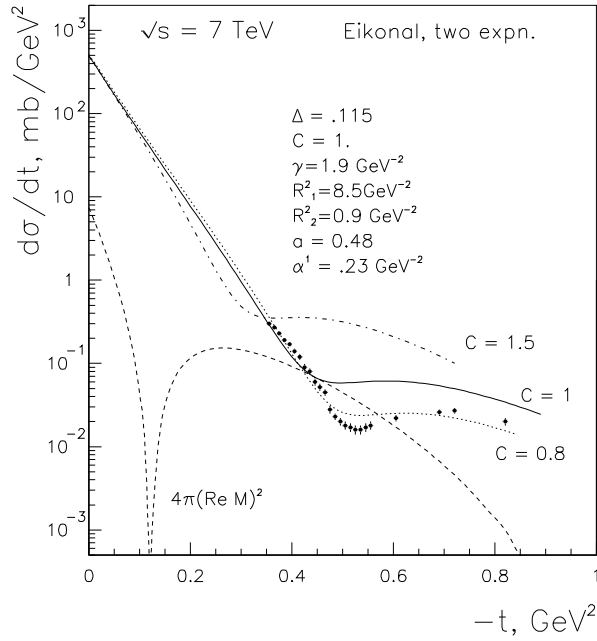


Figure 3: The differential cross section of elastic  $pp$  scattering at  $\sqrt{s} = 7$  TeV calculated in the eikonal approach,  $C = 1$  (solid curve), and the contribution to differential cross section of elastic  $pp$  scattering at  $\sqrt{s} = 7$  TeV of only the real part of the amplitude (dashed curve) by using the two-exponential parametrization of the function  $\gamma(q^2)$  given in Eq. (10). The results obtained for the differential cross section in the two quasi-eikonal approaches with  $C = 1.5$  and  $C = 0.8$  are also shown. The experimental points have been taken from [12].

The results of the calculation of  $d\sigma/dt$  at  $\sqrt{s} = 7$  TeV obtained with the parametrization of the function  $\gamma(q^2)$  given in Eq. (10) are presented in Fig. 3. The quasi-eikonal case in which  $C = 1.5$  leads again to a too fast decrease and it gives a too small slope at low  $q^2$ . Instead, the eikonal approach,  $C = 1$ , leads to a reasonable description of the data. The agreement of our calculations with the experimental data [1] at small  $q^2$  comes from the facts that both the calculated and the experimental  $q^2$ -dependences are close to Gaussians and that the calculated value of  $\sigma^{tot}$  is in agreement with the experimental result [1] (see below). One important point to be stressed is that in the diffraction minimum, or in the beginning of the “shoulder”, the cross section  $d\sigma/dt$  is practically determined by only the real part of the amplitude (see solid and dashed curves in Fig. 3).

The solid curve in Fig. 3 was calculated with the following values of the parameters:

$$\begin{aligned}\Delta &= 0.115, \quad \alpha'_p = 0.23 \text{ GeV}^{-2}, \quad \gamma = 1.9 \text{ GeV}^{-2}, \\ a &= 0.48, \quad R_1^2 = 8.5 \text{ GeV}^{-2}, \quad R_2^2 = 0.9 \text{ GeV}^{-2}.\end{aligned}\tag{12}$$

The quality of the description is even better in the quasi-eikonal case with  $C = 0.8$ . However, value of  $C$  smaller than 1 seem to be in contradiction with the Reggeon unitarity condition [13].

The differential cross section of elastic  $\bar{p}p$  scattering at  $\sqrt{s} = 62 \text{ GeV}$ ,  $\sqrt{s} = 546 \text{ GeV}$ , and  $\sqrt{s} = 1.8 \text{ TeV}$  calculated with the values of the parameters given in Eq. (12) are presented in Fig. 4. At the energy  $\sqrt{s} = 62 \text{ GeV}$  the theoretical curves are slightly below the experimental points, probably due to the contribution of the  $f$ -Reggeon exchange, that has not been accounted for in our calculations.

The calculated values of total cross sections  $\sigma^{tot}$ , of  $d\sigma/dt(t=0)$ , and of the slope of the elastic scattering cone parameter  $B_{el}$  ( $d\sigma/dt \sim \exp(-B_{el} \cdot q^2)$ ) are presented in Table 1, together with the experimental data. It is necessary to note that the slope parameter was calculated in the interval  $q^2 = 0 - 0.1 \text{ GeV}^2$ .

$\sqrt{s}$	$\sigma^{tot}$ (mb)	$d\sigma/dt(t=0)$ (mb/GeV <sup>2</sup> )	$B_{el}$ (GeV <sup>-2</sup> )
546 GeV	60.6	191	16.7
[21]	$61.9 \pm 1.5$	-	-
[22]	$61.3 \pm 0.9$	$196 \pm 6$	$15.35 \pm 0, 19$
1.8 TeV	76.2	301	18.6
[22]	$80.0 \pm 2.2$	$335 \pm 19$	$16.98 \pm 0, 25$
[23]	$71.7 \pm 2.0$	-	-
7 TeV	97.6	493	21.2
[1]	$98.3 \pm 2.8$	-	$20.1 \pm 0, 4$

Table 1. The comparison of the calculated values of total cross sections  $\sigma^{tot}$ , of  $d\sigma/dt(t=0)$ , and of the slope parameter  $B$  with the corresponding experimental data [1, 21, 22, 23].

The general energy dependence of the differential elastic  $pp$  ( $\bar{p}p$ ) cross sections is shown in Fig. 5. At the energy  $\sqrt{s} = 62 \text{ GeV}$  some contribution of  $f$ -Reggeon should be present.

However, in the complete Reggeon diagram technique [6] not only Regge-poles and cuts, but also more complicated diagrams, e.g. the so-called enhanced diagrams, should be taken into account. In the numerical calculation of such diagrams some new

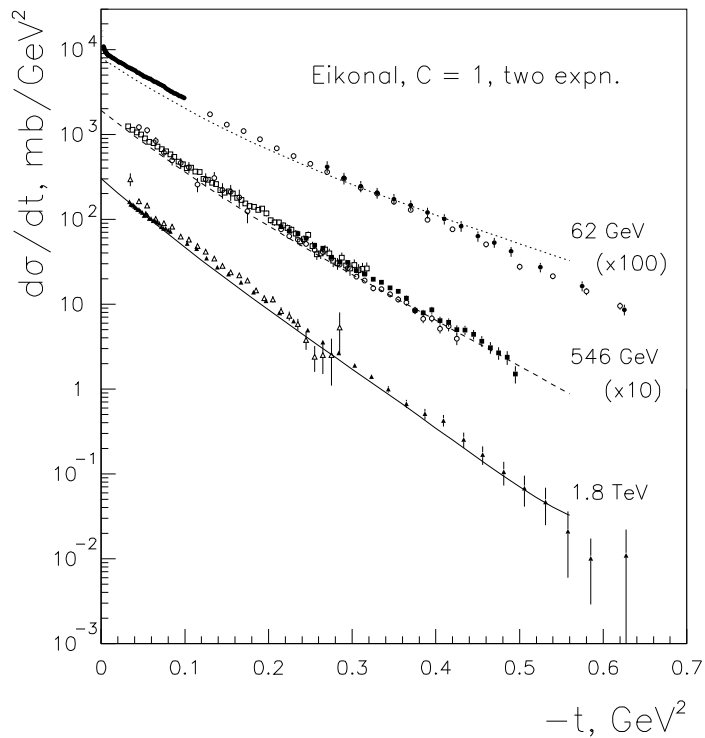


Figure 4: The differential cross section of elastic  $\bar{p}p$  scattering at  $\sqrt{s} = 62$  GeV, [14, 15, 16]  $\sqrt{s} = 546$  GeV [17, 18, 19], and  $\sqrt{s} = 1.8$  TeV [20, 22] calculated in the eikonal ( $C = 1$ ) approach with the two-exponential parametrization of the function  $\gamma(q^2)$  given in Eq. (10).

uncertainties appear, since the vertices of the coupling of multiregion systems are unknown. The common feature of such calculations results in the additional increase of the Pomeron intercept  $\alpha_P(0) = 1 + \Delta$ .

## 4 Conclusion

We obtain a general description of elastic  $pp$  scattering that seems to be successful, as one can see from Figs. 3 and 4, and from Table 1. To do so we only use the three parameters shown in Eq. (12), namely  $\gamma$ , which determines the normalization of total  $pp$  cross section,  $\Delta$ , which determines the increase of the total  $pp$  cross section with energy, and  $\alpha'_P$  which determines the increase of the diffractive slope cone parameter.

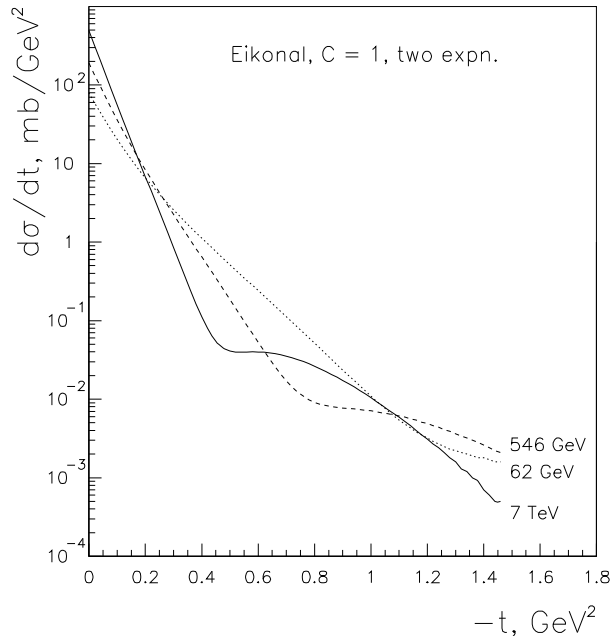


Figure 5: The differential cross section of elastic  $pp$  scattering at  $\sqrt{s} = 7$  TeV (solid curve),  $\sqrt{s} = 546$  GeV (dotted curve), and  $\sqrt{s} = 62$  GeV (dashed curve) calculated in the eikonal approach ( $C = 1$ ) with the two-exponential parametrization of the function  $\gamma(q^2)$  given in Eq. (10).

These parameters are practically not correlated. Another three parameters,  $a$ ,  $R_1^2$ , and  $R_2^2$  are related to the geometrical shape of the proton and they should be determined from the experiment in the same way as we determine the geometrical shape of atomic nuclei.

The exact values of the position of the diffractive dip and of the elastic cross section in the dip-region strongly depend of the particular form, like those in Eqs. (8) and (10), chosen to parametrize the  $q^2$ -dependence of the Pomeron-nucleon coupling. With our oversimplified parametrization we did not succeed in describing the dip-region. On the other hand, it is sure this can be done by using a more complicated vertex  $\gamma(q^2)$  with a larger number of parameters, as the parametrization used in [3], and that, strangely enough, shows a minimum at  $b_t = 0$ , or the one in Eq. (11c) of reference [2], which needs a not well justified additional term in order to describe the dip.

### Acknowledgements

We are grateful to M.G. Ryskin for useful discussions and comments. This paper was supported by Ministerio de Educación y Ciencia of Spain under the Spanish Consolider-Ingenio 2010 Programme CPAN (CSD2007-00042) and by project FPA

2005–01963, by Xunta de Galicia (Spain) and by University of Santiago de Compostela (Spain), and, in part, by grant RFBR 11-02-00120-a.

## References

- [1] G. Antchev et al., TOTEM Collaboration, *Europhys. Lett.* **96**, 21002 (2011).
- [2] A. Donnachie and P.V. Landshoff, arXiv:1112.2485.
- [3] V. Uzhinsky and A. Galoyan, arXiv:1111.4984.
- [4] M.G. Ryskin, A.D. Martin, and V.A. Khoze, arXiv:1201.6298.
- [5] O.V. Selyugin, arXiv:1201.4458.
- [6] V.N. Gribov, *ZhETF* **53**, 657 (1967).
- [7] P.E. Volkovitsky, A.M. Lapidus, V.I. Lisin, and K.A. Ter-Martirosyan, *Yad. Fiz.* **24**, 1237 (1976).
- [8] B.Z. Kopeliovich and L.I. Lapidus, *Sov. Phys JETP* **44**, 31 (1976).
- [9] M. Froissart, *Phys. Rev.* **123** (1961) 1053.
- [10] K.A. Ter-Martirosyan, *Yad. Fiz.* **10**, 1047 (1969).
- [11] K.A. Ter-Martirosyan, *Phys. Lett.* **B44**, 377 (1973).
- [12] G. Antchev et al., TOTEM Collaboration, *Europhys. Lett.* **95**, 1001 (2011) and arXiv: 1110.1385 [hep-ex].
- [13] V.N. Gribov and A.A. Migdal, *Yad. Fiz.* **8**, 1002 (1968).
- [14] N. Kwak et al., *Phys. Lett.* **B58**, 233 (1975).
- [15] U. Amaldi et al., *Phys. Lett.* **B66**, 390 (1977).
- [16] A. Baksay et al., *Nucl. Phys.* **B141**, 1 (1978).
- [17] G. Arnison et al., *Phys. Lett.* **B128**, 336 (1982).
- [18] R. Battiston et al., *Phys. Lett.* **B147**, 385 (1984).
- [19] C. Augier et al., *Phys. Lett.* **B316**, 448 (1993).

- [20] N.A. Amos et al., Phys. Lett. **B247**, 127 (1990).
- [21] M. Bozzo et al., Phys. Lett. **B147**, 392 (1984).
- [22] F. Abe et al., Phys. Rev. **D50**, 5518, 5550 (1994).
- [23] C. Avila et al., Phys. Lett. **B445**, 419 (1999).